A COMPARATIVE EVALUATION BETWEEN FLAT AND TRADITIONAL ENERGY DIRECTORS FOR ULTRASONIC WELDING OF THERMOPLASTIC COMPOSITES

I. Fernandez Villegas[a*], B. Valle Grande[a], H. E.N. Bersee[a], R. Benedictus[a]

[a]*Structural Integrity and Composites Group, Faculty of Aerospace Engineering, Delft University of Technology, Kluyverweg 1, 2629 HS Delft, The Netherlands*
**e-mail address of the corresponding author: I.FernandezVillegas@tudelft.nl*

Keywords: thermoplastic composites, ultrasonic welding, energy directors

Abstract
Energy directors, responsible for local heat generation in ultrasonic welding, are neat resin protrusions traditionally moulded on the surfaces to be welded. This paper evaluates an alternative energy directing solution for ultrasonic welding of thermoplastic composites based on the usage of a loose flat layer of neat resin at the welding interface, referred to as 'flat energy director'. Analysis of dissipated power, displacement of the sonotrode, welding energy and time as well as weld strength compared to more traditional energy directing solutions showed that flat energy directors, which significantly simplify ultrasonic welding of thermoplastic composites, do not have any substantial negative impact in the welding process or the quality of the welded joints.

1. Introduction

Ultrasonic welding is a joining process very well suited for spot welding of thermoplastic composite structures. Among its main advantages are very high processing rates (welding times of several seconds) and straightforward process monitoring, as indicated in [1, 2]. In fact, modern ultrasonic welders provide power and displacement data that can be directly related to the physical phenomena occurring at the joining interface during the welding process [2]. Process monitoring can be used either for quality assessment or as a powerful tool for the definition of optimum processing conditions [3]. In order to concentrate heat generation at the welding interface, energy directors are required in ultrasonic welding. Traditionally, energy directors are matrix resin protrusions on the surfaces to be welded which are subjected to high cyclic strains during the welding process and hence heat up faster than the adherends. Energy directors are traditionally moulded on the surfaces of the composite adherends. This process usually adds an extra step to the manufacturing of the composite parts to be welded. Moreover, the shape, size and number of energy directors need to be optimized in order to achieve high-quality welds [4]. As already shown in recent work by I.F. Villegas [2,3], there is a much more simple solution for ultrasonic welding of thermoplastic composites based on the usage of flat energy directors. A flat energy director is a loose layer of neat resin placed at the welding interface prior to the welding process. Preferential heating of the flat energy director results from the lower compressive stiffness of the neat resin relative to the compressive stiffness of the composite adherends. Flat energy directors have been found to provide high and consistent weld quality [3].

The main goal of the research in this paper is to assess whether the simplicity in manufacturing offered by the flat energy directors has any counteracting effect in the welding process. With this purpose, welding with flat energy directors was evaluated relative to the more traditional solutions depicted in Fig. 1. These were triangular ridges moulded on the surface of one of the adherends (denoted by 4TM hereafter), as proposed by other authors, and triangular ridges moulded on one loose stripe of neat resin (denoted by 4T hereafter), as already used in some of our previous work [5]. Individual thermoplastic composite samples were ultrasonically welded in a lap shear configuration using these three different types of energy directors. Relationships between the feedback of the ultrasonic welder, i.e. power and displacement, and the transformations occurring at the interface were analysed for the three cases and used to define optimum welding parameters. Weld strength, failure modes, welding time and energy were compared and discussed.

Figure 1. Types of energy directors used in this study. Left: four triangular ridges moulded on substrate (4TM); middle: four triangular ridges moulded on a loose resin stripe (4T); right: flat energy director

2. Experimental

The thermoplastic composite used for this research was carbon fibre reinforced polyphenylene sulfide (CF/PPS) with a five harness satin fabric reinforcement, provided by Ten Cate Advanced Composites, The Netherlands. Six-layer laminates with a $[(0/90)_3]_s$ stacking sequence and 1.92 mm nominal thickness were manufactured in a hot platen press at 320°C and 10 bar for 15 min. 101.6 mm-long and 25.4 mm-wide samples were water-jet cut out of these laminates with their longer side parallel to the main apparent orientation of the fibres.

The energy directors were also manufactured in a hot platen press with the processing parameters displayed in Table 1. Note that a temperature below the melting temperature of PPS was used in all cases in order to prevent resin flow and void formation. An aluminium mould with four triangular ridges (spacing 3.25 mm, 90° at the apex of the triangles) was used for the manufacturing of the 4T (four triangular ridges moulded on a loose resin stripe) and 4TM (four triangular ridges moulded on the substrate) energy directors. The size, shape and number of triangular ridges was decided upon based on previous optimization studies. PPS film was used for the manufacturing of the flat and 4T energy directors, whereas PPS powder was used for the manufacturing of the 4TM energy directors. The final dimensions of the energy directors are also displayed in Table 1. During the moulding of the 4TM energy directors, excess resin powder was laid on the mould to ensure a proper connection between the triangular ridges and the substrates. As a result, a resin layer remained between the triangular ridges and the composite, as shown in Fig. 2 and 3. It must be noted that, as Fig. 2 also shows, the 4TM energy directors showed a certain degree of oxidation given away by the somewhat brown colour of the PPS resin. Likewise, they energy featured some porosity caused by insufficient compaction of the PPS powder, as seen in Fig. 3. As shown later on, further compaction was achieved during the welding process.

Individual samples were welded in a single-lap configuration with a 12.7 mm-long overlap using a 20 kHz Rinco Dynamic 3000 ultrasonic welder. This is a microprocessor-controlled welder that automatically adjusts the electrical power input in order to keep a constant amplitude throughout the welding process. A 40 mm-diameter cylindrical titanium sonotrode

was used in this study. A custom-made clamping tool that prevents the samples from shifting and allows for vertical movement of the upper substrate during the squeezing of the energy director out of the welding interface [2,3] was used. Both the flat and the 4T energy directors were cut to the final dimensions and placed between the adherends prior to the welding process and attached to the bottom adherend with adhesive tape. A custom-designed aligning tool was used to ensure that the triangular ridges were parallel to the shortest side of the adherend and always placed in the same location (which coincided with the location of the triangular ridges in the 4TM energy director). The 4TM energy director was already moulded to one of the substrates and thus needed no further fixation. 500 N welding force and 86.2 µm peak-to-peak vibration amplitude were used for all the welds. Solidification force and solidification time were 1000 N and 4 s, respectively. The welding process was displacement controlled, meaning that the duration of the ultrasonic vibration was indirectly controlled through the displacement or travel of the sonotrode [2,3].

ED type	Material	Temperature (°C)	Pressure (bar)	Time @ processing T (min)	Thickness of flat part of ED (mm)	Height of triangular ridges (mm)
Flat	Resin film (0.08 mm thick) – 5 layers	260	20	10	0.4	-
4T	Resin film (0.08 mm thick) – 5 layers	260	20	10	0.4	0.5
4TM	Resin powder	275	10	30	0.25	0.5

Table 1. Processing conditions and geometric features of the different types of energy directors in this study

Figure 2. Triangular energy directors moulded on the surface of the adherends. The darker colour of the PPS resin in the energy directors evidences some oxidation.

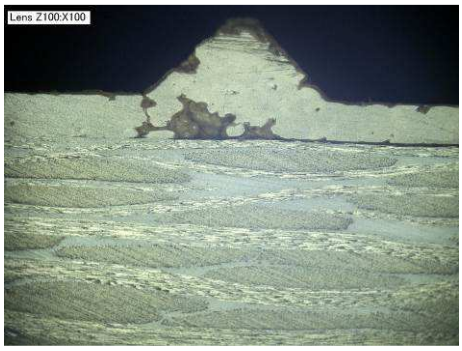

Figure 3. Cross-sectional micrograph of triangular energy director moulded on the surface of the composite adherend.

The welded samples were statically tested according to ASTM D 1002 in a Zwick 250 kN universal testing machine. The apparent lap shear strength of the samples was calculated by dividing the maximum load by the overlap area (i.e. 25.4 mm x 12.7 mm). Five samples were tested per set of welding conditions and average lap shear strength and standard deviation values were calculated. Optical microscopy was used to analyse cross sections of the welded samples. Naked eye was used for the observation of the fracture surfaces.

3. Results and discussion

3.1. Power and displacement curves

The power and displacement curves for the flat energy director case show, as expected, the same features as the ones presented in [2] for ultrasonic welding of CF/PEI composites with flat energy directors. Typical power and displacement curves for welding of CF/PPS samples with 0.4 mm-thick flat energy directors for 100% travel are shown in Fig. 4. As discussed in detail in [2], these curves divide the vibration phase of the process in five distinct stages in which different physical phenomena are observed at the welding interface. In stage 1, characterized by a continuous increase of the power without significant changes in the displacement, heating of the energy director occurs without any observable physical transformations at the welding interface. In stage 2, characterized by a decrease of the power without significant changes in the displacement, the energy director starts to locally melt as a hot-spot nucleation and growth process. In stage 3, characterized by a simultaneous increase of the power and the displacement, the whole energy director is molten and starts to flow. In stage 4, which features a power plateau and increasing displacement, the matrix in the first layer of the adherends starts to melt. Finally, in stage 5, characterized by a power drop and still increasing displacement, melting of the matrix in the bulk of the adherends occurs.

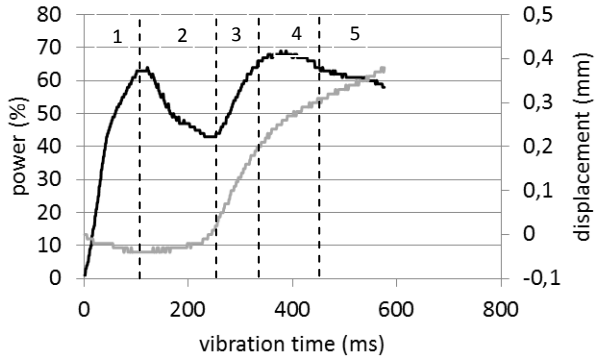

Figure 4. Power (black) and displacement (grey) curves for ultrasonic welding with flat energy directors and different stages in the vibration phase of the welding process (CF/PEI, 500 N welding force, 86.2 µm welding amplitude, 100% travel)

When more traditional, triangular energy directors are used, heating and melting of the energy director first occurs close to the tip of triangles as stated by Benatar and Gutowski in [1], owing to a higher cyclic strain that results from the decreased cross-sectional area, and progresses towards the base of the triangles. Fig. 5 shows how this melting behaviour can be observed in the power and displacement curves for a welding process with 4T energy director (i.e. a resin stripe with four triangular ridges moulded on one side). As indicated in Fig. 5, the vibration phase of the welding process can be now divided into 6 stages. Stage 1' is similar to stage 1 in the case of a flat energy director in the sense that no displacement of the sonotrode is observed and the power increases continuously. It corresponds to the heating of the energy directors which, as mentioned already, is concentrated near the tips of the triangles. Due to the high cyclic strains, the triangular ridges undergo during the welding process as well as the high contact pressure and hence surface friction between the ridges and the adherend, this heating phase is considerably shorter than in the case of the flat energy directors. In stage 2' the triangular ridges gradually melt and, consequently, the displacement of the sonotrode increases in this stage from 0 to 0.4 mm, which is close to the total height of the triangles in the energy director. Since the volume of resin that needs to be heated up to melt increases as the melting process progresses from the tip to the bottom of the triangles, a gradual increase in the power is also observed in stage 2'. In stage 3', the displacement of the sonotrode drastically slows down. This is the stage where the flat part of the energy director progressively melts and hence it is comparable to stage 2 in the flat energy director process.

The main difference is that in the case of the 4T energy directors heating and melting of the flat part of the energy director is already initiated by the four triangular ridges, therefore it is not fully dependent on surface friction [6] and the process is faster. As well as in stage 2 of the flat energy director process, the power drops in stage 3' as a result of a gradual decrease of the area of the flat part of the energy director yet to be heated and melted. Stages 4', 5' and 6' are comparable to stages 3, 4 and 5, respectively. They are therefore characterized by flow of the energy director as a whole and melting of the resin in the uppermost and, later, in deeper layers of the adherends.

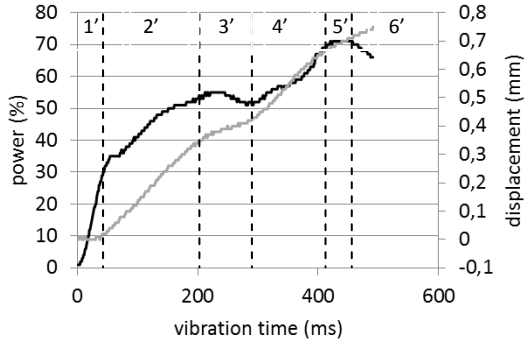

Figure 5. Power (black) and displacement (grey) curves for ultrasonic welding with 4T energy directors and different stages in the vibration phase of the welding process (CF/PEI, 500 N welding force, 86.2 µm welding amplitude, 90% travel)

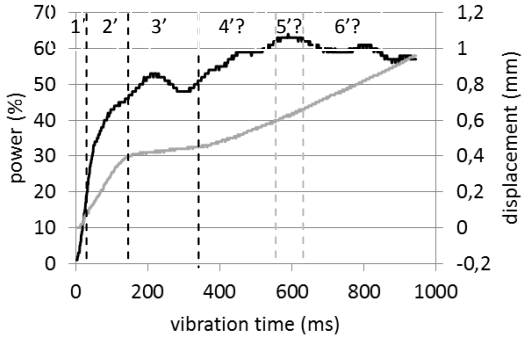

Figure 6. Power (black) and displacement (grey) curves for ultrasonic welding with 4TM energy directors and different stages in the vibration phase of the welding process (CF/PEI, 500 N welding force, 86.2 µm welding amplitude, 105% travel)

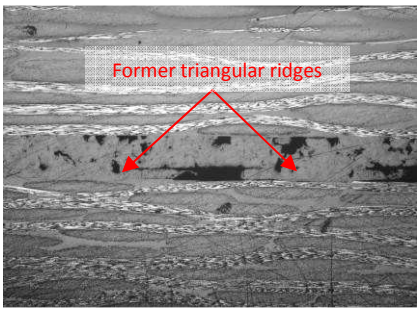

Figure 7. Weldline for 4TM at 0.4 mm travel showing an intermediate step in the melting of the (initially) triangular ridges (500 N and 86.2 µm)

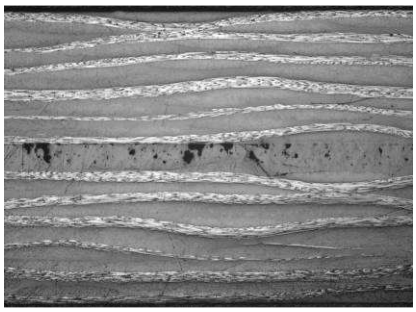

Figure 8. Weldline for 4TM at 0.5 mm travel showing no sign of the (initially) triangular ridges (500 N and 86.2 µm)

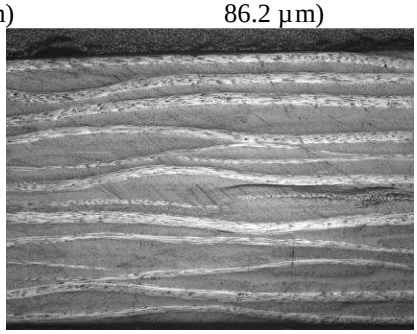

Figure 9. Weldline for 4TM at 0.7 mm travel showing no porosity as a result of the compaction force exerted by the sonotrode during the welding process (500 N and 86.2 µm)

As shown in Fig. 6, the displacement curve for the welds performed with 4TM energy directors (four triangular ridges directly moulded on one of the adherends) is similar to the 4T energy directors displacement curves. The main differences are the shorter duration of stage

1' (initial zero-displacement stage) and a longer duration of stage 3' (significant drop in the displacement increase rate). The shorter duration of stage 1' could be based on the higher ability of deformation of the triangular ridges as a result of the poor compaction of the PPS powder used for the moulded energy directors. The existence of a stage 3' in the displacement curves for 4TM energy directors is related to the presence of a relatively thick layer of resin between the base of the triangular ridges and the surface of the adherend (Fig. 3) owing to the manufacturing process. The fact that this layer of resin is moulded on the adherend and, therefore, is not subjected to surface friction at that interface, makes stage 3' longer than in the case of 4T loose energy directors. The definition of stages 4', 5' and 6' for the 4TM case is challenging owing to the fact that the power curves usually show multiple peaks.

Fig. 7 to 9 illustrate the evolution of the interface at different stages during the welding of 4TM samples through cross-section micrographs. These micrographs show how the triangular ridges are the first features to melt. After that, heat continues to be generated at the interface, which combined with the welding pressure, causes effective compaction of the weldline, and hence a reduction of the initial porosity, and resin squeeze flow.

3.2. Welding output

Based on the power and displacement curves presented in the previous section and on the methodology proposed in [3] for the determination of the optimum welding parameters, optimum travel values (displacement-controlled welding) for the flat and 4T energy director cases were defined (Table 2). Note that, as explained in [3], the optimum travel values for the flat and the 4T energy directors fall within stage 4 (Fig. 4) and stage 5' (Fig. 5), respectively. As discussed earlier, these stages are characterized by melting of the matrix in the uppermost layer of the adherends and simultaneous squeeze flow of the molten energy director. In the case of 4TM energy directors, an optimum travel value was defined from the analysis of the cross sections of welded samples, since the power curves did not allow for a straightforward definition of stage 5'.

Type of energy director	Welding force (N)	Vibration amplitude (µm)	Optimum travel (mm)
Flat	500	86.2	0.30
4T	500	86.2	0.73
4TM	500	86.2	0.75

Table 2. Optimal welding conditions for the different types of energy directors investigated in this work

For each type of energy director, five samples were welded in the conditions indicated in Table 2 and mechanically tested following ASTM D 1002. The apparent shear strength (LSS) as well as the maximum power dissipated during the welding process, energy consumption and vibration times are displayed in Table 3.

Type of energy director	LSS ± standard deviation (MPa)	Maximum power ± std. deviation (W)	Energy ± std. deviation (J)	Vibration time ± std. deviation (ms)
Flat	37.1±1.3	1980±60	801±83	520±58
4T	35.8±1.5	2040±165	866±105	584±89
4TM	17.7±4.6	1890±162	996±49	659±54

Table 3. Output of the welding process for the three different types of energy directors considered in this study (average values for a sample population of 5 for each case)

The results in Table 2 show similar apparent lap shear strength values with similar low scatter for both the flat and the 4T energy director solutions. In these two cases, fracture surfaces show fully welded areas with intralaminar failure and tearing of the fibre bundles as the failure mode, which is associated to the strongest ultrasonic welds [3] (Fig. 10). The maximum power dissipated, welding energy and vibration time are as well very similar in both flat and 4T energy director welding. The similar energy consumed in both cases (only 8% higher in average for 4T case) indicates that heat generation is more efficient when the 4T energy directors are used, as also inferred from the power and displacement curves, where a 20% higher volume of energy director needs to be melted and squeezed out of the welding interface.

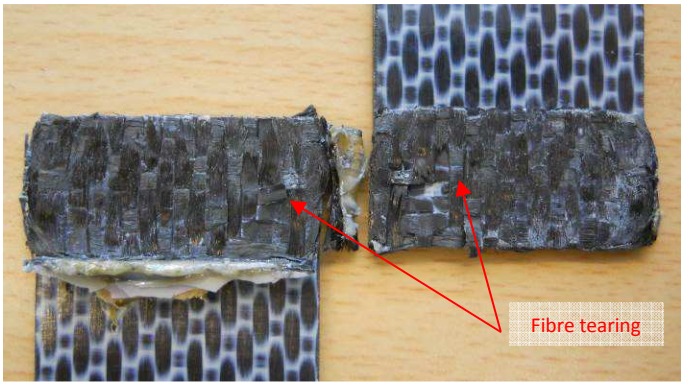

Figure 10. Fracture surface for a 4T welded sample (500 N, 86.2 µm, 0.73mm)

The apparent lap shear strength yielded by the 4TM welds is significantly lower with a much higher scatter. The fracture surfaces of 4TM samples surprisingly show a significant amount of interfacial failure. Fig. 11 presents representative mating fracture surfaces for the 4TM samples. These fracture surfaces indicate that little to no melting occurs on the adhered on top of which the energy director is moulded (Fig. 11, right). Conversely, extensive melting of the matrix with significant deformation of the fibre bundles can be observed in the mating surface fracture (Fig. 11, left). This indicates that the heat generated in the triangular ridges is easily transferred to the adherend they are in direct contact with. On the contrary, the existence of a layer of resin between the ridges and the adherend they are moulded onto serves as an insulator that hinders heat transfer in that direction. Moreover, the lack of surface friction between this layer of resin and the adherend it is moulded to, hampers viscoelastic heating [6] and hence heat generation within the layer. This leads to an unbalanced situation in which one of the adherends is overheated even before the whole energy director is melted and the resin on the surface of the other substrate starts to melt (Fig. 11). This result emphasizes the importance of surface friction when flat energy directors (or energy directors with flat sections) are used at the welding interface. It also suggests that welding with flat energy directors moulded on the adherends might not yield satisfactory results.

Figure 11. Mating fracture surfaces for a 4TM welded sample (500 N, 86.2 µm, 0.75mm)

4. Conclusions

A study on flat versus triangular energy directors for the ultrasonic welding of CF/PPS composites was carried out. The analysis of the feedback provided by the ultrasonic welder showed that in all studied cases similar events in the dissipated power and sonotrode displacement curves could be related to the different steps in the heating, melting and squeeze flow of the energy director as well as heating and melting of the matrix in the adherends. Optimum travel values that led to high apparent lap shear strength levels were easily defined from the power and displacement curves for both the flat energy director and the 4T energy director (i.e. four triangular ridges moulded on a loose stripe of resin) cases. Lap shear strength, welding energy, maximum dissipated power and welding time were similar for the flat and 4T energy director solutions. Moulding of the triangular ridges on top of the adherends for the 4TM energy director solution proved, however, to be challenging and the welding process seemed to be hindered by the presence of a thin moulded layer of resin between the adherend and the triangular ridges.

As the main conclusion of this work, flat energy directors offer much more simplified processing as compared to more traditional solutions with no significant negative impact in the welding process for the specific type of welds considered in this study. Surface friction plays, however, a major role in heat generation when flat energy directors are used. Therefore, hard constraints to the relative movement between the flat energy director and the adherends might have a negative influence in the welding process.

Acknowledgments

The authors would like to thank Ten Cate Advanced Composites in The Netherlands for supporting this research.

References

[1] A. Benatar, T. Gutowski. Ultrasonic welding of PEEK graphite APC-2 composites. *Polymer Engineering and Science*, 29 (23):1705-1721, 1989.

[2] I.F. Villegas. In situ monitoring of ultrasonic welding of thermoplastic composites through power and displacement data. *Journal of Thermoplastic Composite Material*, epub ahead of print 14 Feb 2013, DOI: 10.1177/0892705712475015

[3] I.F. Villegas. Optimum processing conditions for ultrasonic welding of thermoplastic composites. In *International Conference on Composite Materials (ICCM)*, Montreal, Canada, 2013.

[4] H. Potente. Ultrasonic welding, principles and theory. *Materials Design*, 5(5): 228-234, 1984.

[5] I.F. Villegas et al. Process and performance evaluation of ultrasonic, induction and resistance welding of advanced thermoplastic composites. *Journal of Thermoplastic Composite Materials*, 26(8):1007-1024, 2012.

[6] Z. Zhang et al. Study on heating process for ultrasonic welding of thermoplastics. *Journal of Thermoplastic Composite Materials*, 23(5): 647-664, 2010.